



Microclimate analysis of high-density urban residential open enclosures: A case of Thane, India

Vandana Tiwari Srivastava ✉

Department of Architecture and Planning, Madhav Institute of Technology and Science, Gwalior, India

Alok Sharma

Indian Institute of Travel and Tourism Management, Gwalior, India

Sanjay Singh Jadon

Department of Architecture and Planning, Madhav Institute of Technology and Science, Gwalior, India

ARTICLE INFO	ABSTRACT
<p>Received: 29 July 2022 Revised : 04 October 2022 Accepted: 14 November 2022</p> <p>Available online: 09 March 2023</p> <p>Key Words: Built-environment ENVI-met Floor space index Microclimate Simulation Sustainable</p>	<p>Urban heat island produces a significant impact by modifying the microclimate in urban areas. To ensure good quality of life with a safe and healthy built environment, the floor space index (FSI) can be an effective tool. It helps to control the urban densities and shape the morphology of the built environment. Taking the case of typical residential development in a densely populated Indian city, an attempt has been made to explore the relationship between FSI and the microclimate of such open spaces that perform like an open enclosure (OE). Adopting the simulation pathway in ENVI-met, a mathematical relationship is established between an important tool used by urban planners and the variables of the microclimate in a typical urban enclosure. The observations indicate that FSI has a strong negative correlation with air temperature and mean radiant temperature. Evaluation of physiological equivalent temperature reveals a similar relationship with FSI, demonstrating a temporal transposition of the trend for a particular FSI range of 2.5-3.5 in the late evening and early morning hours due to high humidity levels and reduced wind speeds. The study will help the planners to prognosticate the microclimatic variables while working out the data-based, logical and well-evaluated future development control regulations.</p>

Introduction

According to the '2018 Revision of World Urbanization Prospects', by the year 2050, around 68% of the world's population will live in urban areas and India alone will add around 416 million people to the overall urban dwellers across the globe. Due to the swelling urban densities, the quality of life in urban areas is greatly compromised. The formation of urban heat islands (UHI) has deteriorated the urban environment by modulating the microclimate of the cities. In the recent past, studies related to UHI and urban microclimate have gained much importance worldwide. UHI is the resultant warming of ambient air temperatures (T_{air}) in the urban areas as compared to its rural counterparts due to a variety

of factors that include reduced vegetation, increased material-low albedo surfaces, trapping of radiations due to multiple reflections, urban morphologies, reduced windspeeds and anthropogenic emissions. The fabric of cities has evolved over a while, either organically or with partial/piecemeal interventions or even entirely as a greenfield development. In all cases, the tools used by planners play an important role in shaping our cities. The configuration and orientation of streets, built volumes and the properties of the surfaces are directly linked to the urban climate (Shareef & Abu-Hijleh, 2020). In the process of urbanisation, the cities have transformed into concrete jungles, and small pockets of open spaces that are left within the developed areas are

Corresponding author E-mail: architect.vandanats@gmail.com

Doi: <https://doi.org/10.36953/E.CJ.14092419>

This work is licensed under Attribution-Non-Commercial 4.0 International (CC BY-NC 4.0)

© ASEA

the only places that function as relief zones providing fresh air to breathe, enriching the quality of life, for the people living in their proximity. But due to the presence of UHI the microclimate of these open spaces too, is greatly altered which in turn affects the functionality/use of the open spaces for which they were intended. Improper building bylaws and open space requirements are responsible for heat gain from all sides of the building (Thakur & Sanyal, 2016). The role of urban planners is crucial for achieving good air quality and thermal comfort (OTC). According to the international standard of thermal comfort (ISO 7730:1994), the factors affecting thermal comfort can be classified into two groups, namely, climatic and personal factors. Climatic factors include air temperature (T_{air}), radiation (T_{mrt}), humidity and wind speed (WS), whereas personal factors are the rate of metabolism of the human body and insulation due to clothing. The studies conducted in the past to understand the relationship of the elements of the cityscape, with the microclimate can be categorized under the following major heads. Large-scale urbanization has resulted in the loss of green cover in the cities which in turn is responsible for the loss of habitat for many species, increase in the pollution of natural resources and deterioration of the quality of life of the city dwellers (United Nations). Vegetation helps to mitigate the impact of climate change in urban areas (Tumini & Rubio-Bellido, 2016). It helps to control the microclimate by decreasing T_{air} , increasing humidity and modulating the wind ventilation (Nasir *et al.*, 2015). The tree cover ratio is found to be negatively related to daytime UHI (Lin *et al.*, 2017). Roadside plantations can cool the microclimate near building facades by up to 0.25-1.28°C (Chatzinikolaou *et al.*, 2018). Urban geometry plays an important role in formulating the microclimate of built and unbuilt areas by modifying the duration of exposure of surfaces to the solar radiations, in terms of sky view factor (SVF) (Jamei *et al.*, 2017). Shading reduces the amount of light that reaches building surfaces and pavements, reducing the reflected light, thermal radiations and surface temperatures (Erell *et al.*, 2011). Shading is a function of aspect ratio that can be achieved by placing the buildings in close proximity and orienting streets north-south

(Emmanuel *et al.*, 2007). A case study of a superblock in Jakarta concluded that the comfort conditions surrounding a high-rise building were worse with minimal diurnal variations as compared to the central park area (Donny Koerniawan, 2015). Urban areas are characterized by increased material surfaces. These surfaces absorb more radiation and are responsible for increased ambient T_{air} , depending on their material and colour (Mehrotra *et al.*, 2021). Therefore, optimization of material selection can substantially improve thermal comfort (Kakoniti, Georgiou, Marakkos, Kumar, & Neophytou, 2016). High albedo materials in a high-density commercial area, were found to reduce surface temperature up to 5-6°C (Emmanuel *et al.*, 2007). Using reflective materials on pavements helps to improve thermal conditions (Santamouris *et al.*, 2012). But the benefit is reduced due to the reflected solar radiations being trapped in the built environment, thereby, increasing T_{air} and cooling loads (Chatzidimitriou & Yannas, 2016; J. Yang, Wang, & Kaloush, 2015). Thermal comfort conditions are negatively related to the sky view factor of high albedo material surfaces (Salata, Golasi, Vollaro, & Vollaro, 2015). Several microclimate simulation and prediction software tools with different levels of complexity are available. In a comparative study, ENVI-met was found to be most suitable to simulate thermal comfort indices, based on the fundamental laws of fluid dynamics and thermodynamics. It is a user-friendly tool to predict meteorological parameters and evaluate design strategies in outdoor spaces (Albdour & Baranyai, 2019). It has been used by several researchers in the past. A study conducted by Kakon *et al.* (2009) to investigate the impact of development rules on the microclimate of urban canyons in Dhaka, (Kakon *et al.*, 2009), and another study by Du *et al.* (2018) examined the influence of building heights and porosity on the wind comfort, around various building configurations in Hong Kong, (Du *et al.*, 2018), and study by Stocco *et al.* (2021) to evaluate various design alternatives of an urban square in Mendoza Argentina to achieve the best conditions of thermal behaviour and comfort (Stocco *et al.*, 2021) are some of the similar studies done in the past using ENVI-met as the simulation tool. Using measured data as full forcing ENVI-met produces

realistic results with good accuracy (Ketterer&Matzarakis, 2015; X. Yang, Zhao, Bruse, & Meng, 2013). Development Control Regulations (DCR as per local authority) applies various tools to control the development in urban areas and thereby maintain an equitable distribution of infrastructure facilities, and open spaces and ensure a healthy built environment for all. It is important to understand the relationship of various tools of DCR with the microclimate of built and unbuilt areas of the city fabric. The relationship shall provide inputs to optimize the urban morphology in the development plans and formulate mitigation strategies as DCR thereby reducing UHI (Smith & Levermore, 2008; Yahia & Johansson, 2013). As per the local DCR of the study area, the provision of open space is a function of the area of the land parcel, available for development, therefore as the permissible floor space index (floor space index or FSI is the ratio of the total built-up area divided by the plot area available for the development. It is also known as FAR or floor area ratio at many places) increases a greater number of floors are added in the same building and layout plan, to consume the full FSI available. The research aims to understand and analyse the relationship of the floor space index (FSI) with the variables of the microclimate of a typical OE, taking the case of the current trend of housing development in the study area of Thane city.

Material and Methods

The methodology for the present research is based on the simulation method adopted by many researchers using ENVI-met software (Yahia & Johansson, 2013), (Kakon *et al.*, 2009), (Chatzidimitriou & Yannas, 2004). The 3D models of various scenarios of the case studies with varying FSI were constructed. The validation of the models is done by comparing the simulation results of the 3D model of the existing scenario with the microclimate variables recorded on-site in the case studies. The simulation is performed using meteorological data from the nearest weather station. Further, the readings of the variables which constitute the microclimate are recorded at various locations in the 3D models. Statistical analysis of the results of the simulation is conducted to understand the relationship of each microclimatic

variable with the FSI. The mean values of the data recorded at various receptors (the number of receptors placed are; CS1-7, CS2 & CS3-9 each) were used to establish a correlation with the FSI and derive the regression equations for each variable for future applications. In this study, thermal comfort is evaluated based on two climatic factors, specifically, air temperature (T_{air}) and mean radiant temperature (T_{mrt}), along with wind speed (WS) and relative humidity (RH). In a tropical climate, physiological equivalent temperature (PET) is the most commonly used OTC index to assess the value of thermal comfort in outdoor spaces (Fong *et al.*, 2019; Koerniawan, 2017). Therefore, to understand the response of an average person to the thermal environment, PET is used for evaluation.

Study area

The study area lies in Thane (Maharashtra), the most populous district of India, and is currently facing an influx of population as a result of its locational advantage, of adjacency to the megacity of Mumbai. The need to accommodate more people in the limited area of the city boundaries has resulted in increased FSI (also called Floor area ratio FAR) and reduced vegetated unbuilt areas. In high-density residential development, there is a trend of providing central open spaces surrounded by peripheral built structures on all sides. This works as an enclosure for the central open space and the morphology of the surrounding built structures plays an important role in modulating the microclimate and usability of the central open areas. In the first phase 50 housing societies (Figure 2) based on visual analysis of the formation of OE in the layout plans, were selected, mostly located off-Ghodbunder road, which is the main focus of the new development. Further, for the second phase, keeping 20.99% cut/void in the perimeter of the enclosure as the criteria 20 societies were selected, out of which 3 societies (Figure 1) from the middle range were finalized for simulation and analysis, the required physical parameters of the selected case studies are as given in Table 1.

Climate: Thane has a tropical monsoon type of climate that borders on a tropical wet and dry climate. The monthly mean temperature varies from 22°C to 36°C. In winter, the temperature can fall to

Figure 1: Location plan of 50 Housing Societies selected in Phase 1 (Source: Google Earth Satellite Image 2021)

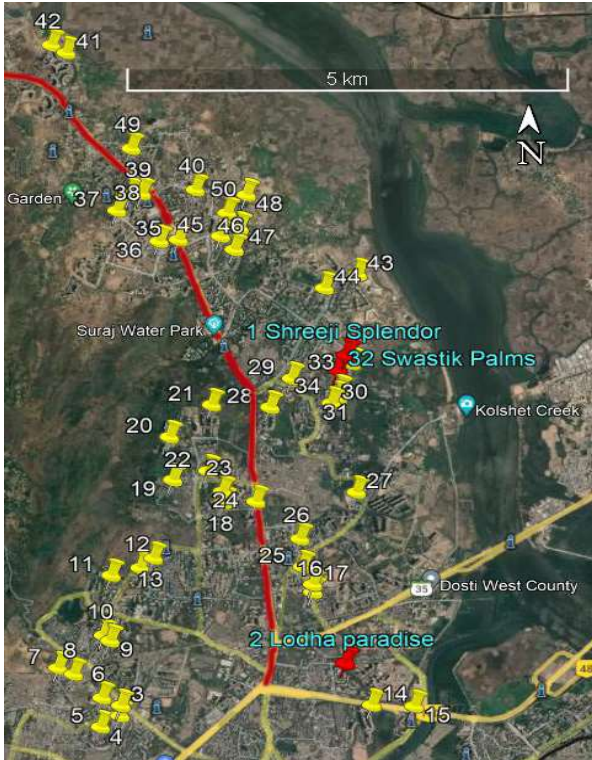


Table 1: Statistical data related to the selected case studies

CS. No.	Total area in sqm	Central open space in sqm	Open enclosure (OE) dimensions		
			Area	Perimeter	Cut/Void
CS1	22968	2853	4984	315	44
CS2	19600	3712	7888	356	48
CS3	21868	2688	6216	316	52

12 °C at night, while in summer it can rise to over 40°C at noon. The monthly average RH ranges from 53% to 90%. The annual range of WS lies between 1 to 3 m/s. Since the impact of UHI is more prominent in summer, therefore, 3rd May 2021, which lies in peak summer, is selected for on-site data recording and simulation.

Model Validation

The existing scenario (Figure 2) with OE and existing vegetation of 3 case studies, was

constructed in ENVI-met spaces using common parameters of, dx =2.0m, dy =2.0m, base dz =3.0m, where 3m of dz, represents the floor-to-floor height as per the prevailing practice in multi-storied housing complexes. The grid cell dimension of 2m x 2m was used to achieve optimum time for simulation and also maintain a realistic level of detail for the ENVI-met model (Salata *et al.*, 2016) with vertical grid generation as equidistant and the lowest cell split into 5 sub-cells. The material for walls and roofs was taken as default wall and default roof with moderate insulation. The discrete model geometry of individual cases is as per Table 2. The microclimate was simulated using full forcing of climatic data; for air temperature, relative humidity, direct SW radiations, diffuse radiations, wind speed and direction retrieved from historic weather data for the selected day for Thane, retrieved from <https://www.meteoblue.com>, accessed on 12th September 2021 and using IND_Mumbai.430030_ISHRAE.epw, available on <https://energyplus.net/weather>. The results of the simulation for T_{air} and humidity were validated with the on-site observations. The microclimate variables of T_{air} and RH were recorded using a dry and wet bulb hygrometer (Table 3). The percentage of RH was calculated with the help of an online interactive psychrometric chart at flycarpet.net, for the corresponding dry and wet bulb temperature (DBT and WBT) readings. The T_{air} and RH were recorded at 11:00, 14:00, 17:00 and 22:00 at one of the receptor locations in each case study (Table 3), at a height of 1.5m from ground level, in the OE and validated with the on-site readings which were recorded at the same location, with the help of hygrometer. According to the correlation coefficient (Table 4) for the simulated and on-site readings of T_{air} and RH, it is concluded that the simulation results have a fairly strong correlation with the on-site observations, with slight variations, which can be attributed to the difference in geometries and other morphological details between the model constructed in ENVI-met and on-site scenario. In the model constructed, only the vegetation, ground surface finishes and built volumes are considered.

Construction of scenarios

To understand the impact of changed FSI regulations on the microclimate of central open space in a typical layout, four scenarios (Figure 3)

were constructed for each case study, in ENVI-met spaces, with the same layout plan, grid dimensions,

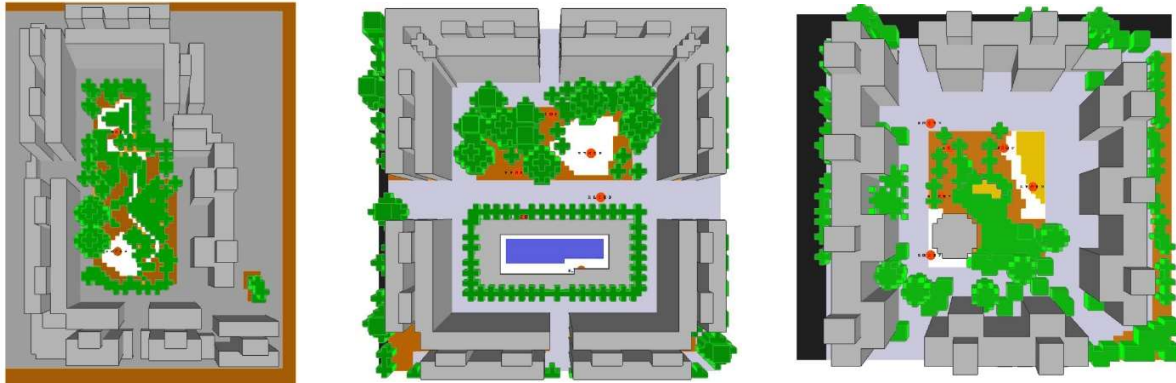


Figure 3: 3D- models of the existing scenario of case studies 1, 2 and 3 (from left to right) constructed in ENVI-met spaces 4.4.6

Table 2: Discrete parameters of 3D-model geometry for case studies

	Grid dimensions	Core xy domain size	Nesting grids	Highest building in the domain	Height of 3D model
CS1	66 x 87 x 30	132.00m x 174m	5	30m	90m
CS2	70 x 70 x 30	140.00m x 140m	7	28m	90m
CS3	77 x 71 x 30	154.00m x 142m	7	30m	90m

Table 3: On-site hygrometer readings for CS1, CS2 & CS3, on 3rd May 2021

Time of recording	Case study 1		Case study 2		Case study 3	
	DBT	WBT	DBT	WBT	DBT	WBT
11:00	34	28	34	26	33	27
14:00	35	28	35	28	34	27
17:00	35	30	35	30	34	29
22:00	33	29	33	25	29	26

Table 4: Comparison of on-site recorded data with simulation results of the existing scenario

Time of recording→			11:00	14:00	17:00	22:00	Correlation coeff.
CS1	T _{air} in °C	Simulation	39.12	39.62	34.67	26.94	R=0.727
		Recorded	34	35	35	33	
	RH%	Simulation	28.72	33.55	37.82	82.49	R=0.806
		Recorded	63.3	58.6	69.3	74.1	
CS2	T _{air} in °C	Simulation	38.60	39.50	34.78	26.89	R=0.754
		Recorded	32	35	35	29	
	RH%	Simulation	30.81	33.40	37.59	82.68	R=0.762
		Recorded	62	58.6	69.3	72.2	
CS3	T _{air} in °C	Simulation	28.56	32.42	36.82	26.92	R=0.759
		Recorded	33	34	34	29	
	RH%	Simulation	28.56	32.42	36.82	82.51	R=0.899
		Recorded	62.6	57.9	68.8	78.7	

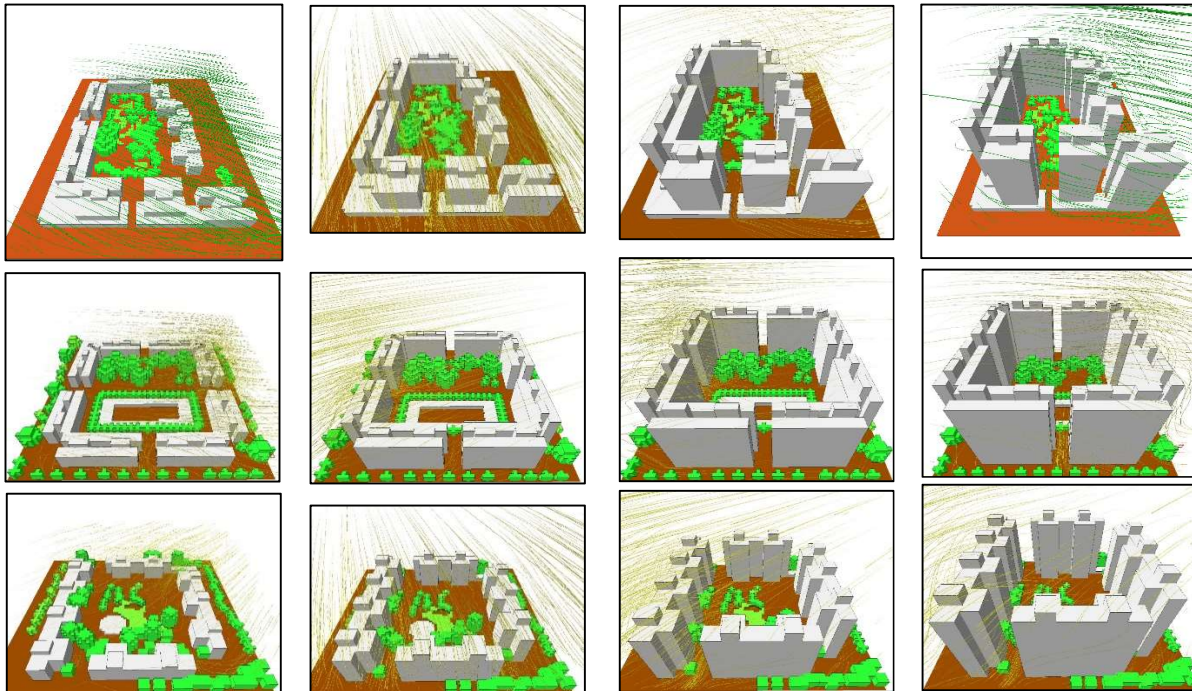


Figure 3: Physical models created in ENVI-met Spaces 4.4.6 for case studies CS1(Top row), CS2 (Middle row), CS3 (Bottom row) and their FSI scenarios respectively, SCN 1,2,3&4 (left to right)

core xy domain size, nesting grids and grid cell dimensions as in existing scenario. The overall height of the built structures under various scenarios is as per the observed trend of development which is a reflection of local firefighting regulations. The physical parameters of various scenarios are as per Table 5. The 3D models of all the scenarios were simulated for 24 hours, starting at 00:00 hrs. All the variables were evaluated at the x/y cut at level k=2 in ENVI-met, which is at 1.5 m from ground level and corresponds to the average height at which the microclimate is experienced. The OTC index of

PET was calculated in Bio-met with the values for the average Indian male of 35 years, a height of 1.65m and a weight of 70kg. Clothing value was taken as 0.5clo considering light summer clothing, walking speed as 1.21 m/s and work metabolism of 80W of light activity. For analysis, daytime is considered as between 06:00 to 19:00 as per the sunrise and sunset on simulation day (Figure 4).The simulation was done in ENVI-met core, using full forcing with the climatic data identical to the existing scenario. Simulation results were then analysed in Leonardo and Bio-met.

Table 5: Physical parameters of constructed FSI scenarios

Case study →				CS1	CS2	CS3
Total land under development in sqm →				16400	19600	16600
Building footprint in sqm →				4196	4908	4252
Scenario	FSI	No. of floors	Max. height	BUA	BUA	BUA
SCN1	0.75	4	12	16605	19845	16808
SCN2	1.5	8	24	33210	39690	33615
SCN3	2.5	13	39	55350	66150	56025
SCN4	3.5	18	54	77490	92610	78435

Note: The actual built-up areas under the scenarios may vary depending upon the detailing and type of architectural spaces created on the individual floor plates. The floor-to-floor height is considered as 3m

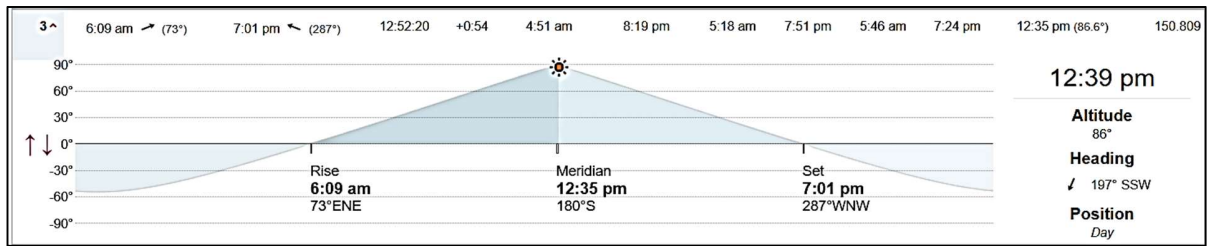


Figure 4: Sun positions on 3rd May 2021 retrieved from www.timeanddate.com

Results and Discussion

The simulation output was recorded at the strategically located receptors, which represent the overall microclimate of the OE. The selected parameters of T_{air} , T_{mrt} , PET, RH and WS, were noted and the mean values of all receptors were considered for further statistical analysis. The values of all the variables were found distorted for the initial and the last hour of the simulation, hence they were reproduced via the interpolation method for analysis. The relationship of microclimatic

variables is first analysed individually with the FSI and then a comparative study was conducted to understand the relative impact of FSI on these parameters. A summary of per-floor variation in the microclimatic parameters corresponding to FSI represented by the scenarios is presented in Table 6. FSI vs T_{air} (Figure 5): Simulation results revealed that during the entire day the impact of FSI on T_{air} was maximum at 14:00 hrs (Figure 6) when the overall reduction in mean T_{air} of SCN 4 was found to be $-0.77^{\circ}C$ less as compared to SCN 1.

Table 6: Summary of per-floor variation in microclimate parameters against FSI scenarios

Category→	FSI 0.75 to 1.5	FSI 1.5 to 2.5	FSI 2.5 to 3.5	FSI 0.75 to 3.5
Change in category →	Low-rise to Mid-rise	Mid-rise to Small high-rise	Small to Big high-rise	Low rise to Big high-rise
No. of floors →	4 to 8 floors	8 to 13 floors	13 to 18 floors	4 to 18 floors
DAY TIME				
$\Delta T_{air}^{\circ}C$	-0.043	-0.029	-0.029	-0.033
$\Delta T_{mrt}^{\circ}C$	-1.327	-0.816	-0.637	-0.898
$\Delta PET^{\circ}C$	-0.480	-0.346	-0.269	-0.357
ΔWS	-0.029	-0.015	-0.003	-0.014
$\Delta RH\%$	-0.021	0.011	0.057	0.018
NIGHT TIME				
$\Delta T_{air}^{\circ}C$	-0.030	-0.022	-0.020	-0.023
$\Delta T_{mrt}^{\circ}C$	-0.109	-0.049	-0.050	-0.067
$\Delta PET^{\circ}C$	-0.070	0.019	-0.001	-0.014
ΔWS	0.018	-0.023	-0.014	-0.008
$\Delta RH\%$	0.405	0.107	0.097	0.189

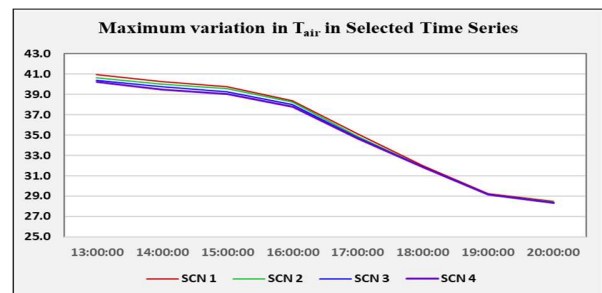
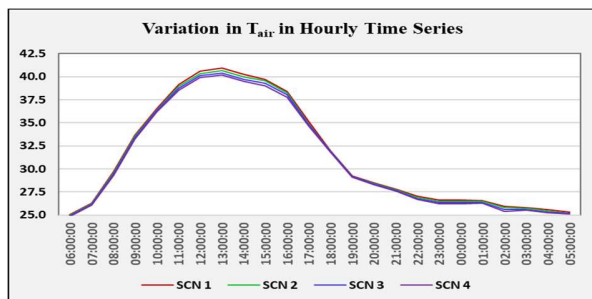


Figure 5: (Left) Chart showing the variation of Mean values of T_{air} at all receptor locations, for hourly time series and Figure 6: (Right) Chart showing maximum variation in T_{air} in selected time series

The minimum impact of FSI was seen in the evening at 19:00 hrs. when the mean T_{air} of SCN 4 was -0.12°C less than SCN 1. The maximum impact of -0.51°C in the nighttime was noted at 2:00 hrs. Overall, for an FSI increase of 2.75 (i.e., from 0.75 in SCN 1 to 3.5 in SCN 4), in the daytime, the average reduction in T_{air} was 0.46°C and in the nighttime, the average decrease in T_{air} was found to be -0.32°C . Therefore, the impact was more pronounced in the daytime. There is a statistically significant relationship ($r= 0.99$, $p= 0.005$) between FSI and T_{air} in $^{\circ}\text{C}$. Overall, FSI is found to have a strong negative correlation with T_{air} . A similar observation was made by Emmanuel *et al.*, in their study related to the H/W ratio. It was observed that the higher H/W ratio tends to decrease T_{air} (Emmanuel *et al.*, 2007). Since higher FSI results in a high H/W ratio, therefore, it will also tend to lower T_{air} . Another study concluded that the high-density urban morphology if well planned can lead to improvement in thermal comfort in tropical climates (Xue *et al.*, 2017).

Since high FSI is associated with high density, therefore, the present study is in agreement with the findings of previous research. Impact of UHI on T_{air} (Figure 7): Study of the scatter plots of change in T_{air} (ΔT_{air}) of the simulation results against the T_{air} of the inflow boundary condition of weather data, for 24 hrs time series, it is found that when the inflow T_{air} is higher, ΔT_{air} is also more. Therefore, when the UHI is more prominent at the city level, i.e. the inflow T_{air} is higher, its impact will be further pronounced ($R^2 = 0.54$) at the micro level, especially when the type of development is low rise and midrise. When the typology of development changes from midrise to high-rise the impact of high UHI is lesser ($R^2 = 0.48$) on the microclimate. Hence the study supports the argument that the higher FSI helps to reduce the impact of UHI by lowering the T_{air} . FSI vs T_{mrt} (Figure 8): It was observed that during the entire day the maximum impact of FSI on T_{mrt} was noted at 16:00 hrs. (Figure 9), when it was found to be -26.22°C less in SCN 4 as compared to SCN 1.

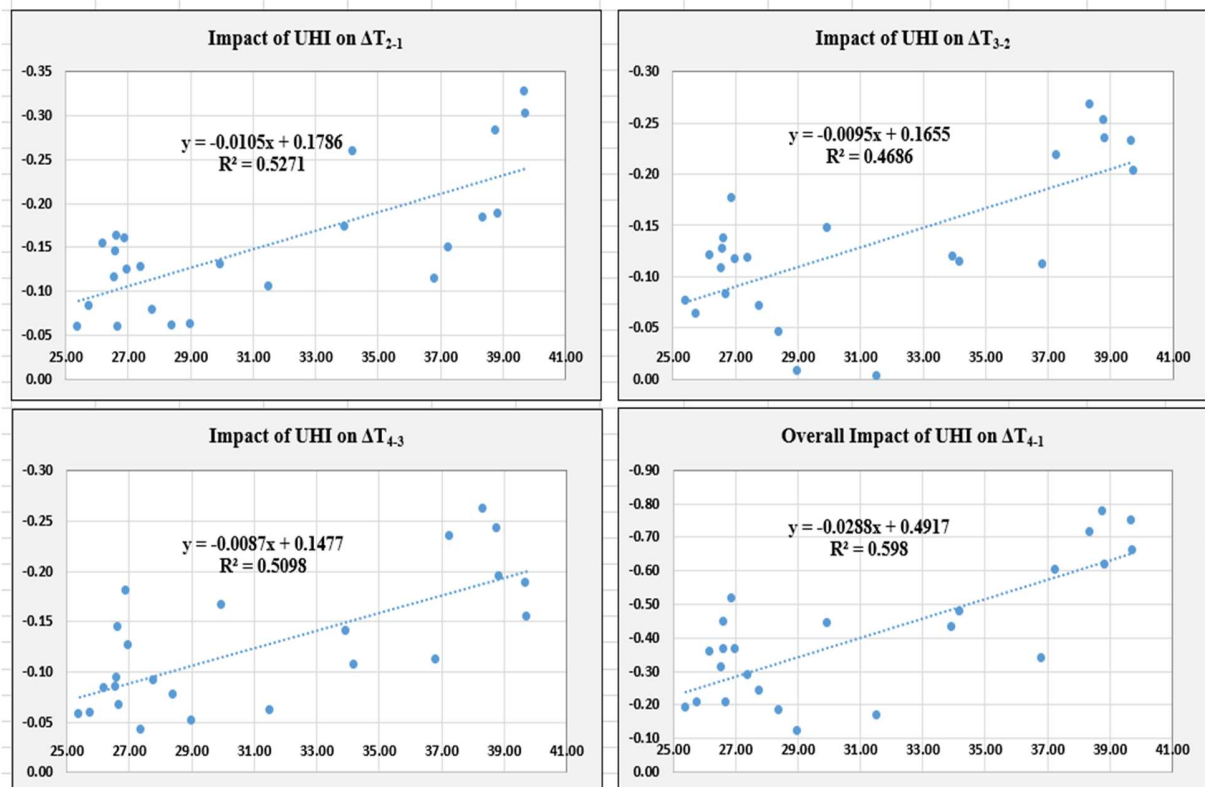


Figure 7: Scatter plots showing the impact of UHI on T_{air} (clockwise from the top left) change in SCN 1 to SCN 2, SCN 2 to SCN 3, SCN 1 to SCN 4 and SCN 3 to SCN 4

The minimum impact of FSI was observed at 23:00 hrs. when the values of SCN 4 were found to be -0.69°C less than the value in SCN1. In the nighttime, a maximum reduction of -1.21°C in T_{mrt} was observed at 2:00 hrs., from SCN 1 to SCN 4. It was observed that, for an increase of 2.75 in the FSI, the average reduction in T_{mrt} was -12.57°C in the daytime, whereas, in the nighttime, the average reduction was -0.93°C . There is a statistically significant relationship ($r= 0.98, p= 0.015$) between FSI and T_{mrt} in $^{\circ}\text{C}$. Therefore, T_{mrt} is strongly negatively correlated to FSI, the impact being maximum at 16:00 hrs. In the absence of direct radiation at nighttime, the overall impact is much less. The results of the present study were found to be in close agreement with a similar study

conducted to understand the impact of building regulations in Chennai (Salal Rajan & Amirtham, 2021). To compare the values in both cases, a reduction in T_{mrt} with the SVF was calculated. It was found that in the present study for every 0.1 reduction in SVF, the T_{mrt} was reduced by -12.48°C , whereas in the case of the previous study, for a reduction of 0.1 in SVF the T_{mrt} was reduced by 11.65°C . Since Mumbai and Chennai both are coastal cities separated by a latitudinal distance of around six degrees, have similar climatic conditions. FSI vs WS (Figure 9): In the statistical analysis it was observed that the resultant windspeed is highest in SCN1 when the building heights are 12m and the FSI was 0.75.

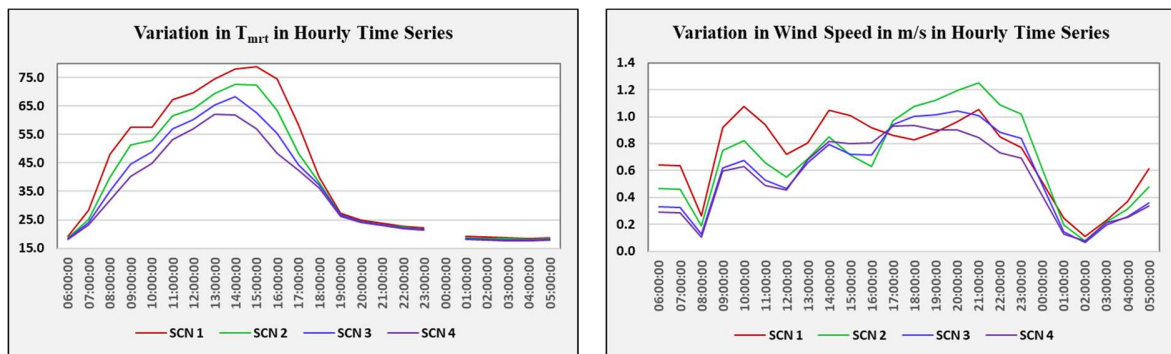


Figure 8: (Left) Chart showing a scenario-wise variation of Mean values of T_{mrt} at all receptor locations, in hourly time series and Figure 9: (Right) Chart showing scenario-wise comparative WS variation in hourly time series

As compared to the wind inflow boundary condition measured at 10 m, the WS measured at 1.5 m was much less. It was observed that as the FSI increases from SCN1 to SCN4 (Figure 9) the windspeed reduction is significant. The maximum impact of FSI in terms of WS modulation was observed at 11:00 hrs when the WS is reduced by -0.455m/s from SCN1 to SCN4. During the entire day, the minimum impact was observed at 19:00 hrs. when the reduction in WS was -0.17m/s . Further observing the variation in windspeed among scenarios it was found that when the building typology changes from low-rise to mid-rise there is a decrease in wind velocity from 17:00 hrs. till midnight when the inflow boundary conditions of WS is highest in the entire day. This trend is negligible when the building typology

changes from mid-rise to high-rise. Further when the typology of the building changes from high-rise to big high-rise the reduction in wind speed is observed in the afternoon till 16:00 hrs and then a marginal reduction between 2:00 to 3:00 hrs in the late night. A similar trend of the reduction in wind speed was reported in a previous study in severe cold regions of China (Jin *et al.*, 2017). Considering the average change in the WS it was noted that the average reduction of -0.09 m/s in WS was the maximum between SCN2 and SCN3 when the building typology changed from mid-rise to high-rise, which supports the findings of a previous study that the midrise enclosed layout shows the worst performance in terms of wind speeds (Ma & Chen, 2020). FSI vs RH (Figure10). It was observed that the variation in RH across the

constructed FSI scenario is nominal. However, there is an average increase of 1.25% RH from SC1 to SCN4, ranging from a maximum of +5.3% at 23:00 hrs. to a minimum of +0.02% at 19:00 hrs. Across the scenarios, the maximum increase in RH was noted between SCN1 and SCN2 when the typology of development changed from low-rise to mid-rise. The average increase in RH in the daytime is less than in the nighttime. As per the analysis, the average increase in RH in the daytime is 0.26% as compared to the average increase of RH of 2.64% in the nighttime. FSI vs PET(Figure11): The urban form has a noticeable

impact on PET (Othman &Alshboul, 2020). From the analysis, it is seen that as the FSI increases from scenario SCN1 to SCN4, the comfort condition improves which is demonstrated by lower mean values of PET. The maximum impact is observed at 16:00 hrs. when the PET in SCN4 is 10.03⁰C lower as compared to SCN1, whereas the least impact was observed at 21:00 hrs. when the PET in SCN4 was higher by 0.013⁰C than in SCN1. The impact of increased FSI is found to be more significant in the daytime with a reduction of -4.99⁰C in the average values of PET from SCN1 to SCN4 as compared to the nighttime reduction of -0.19⁰C.

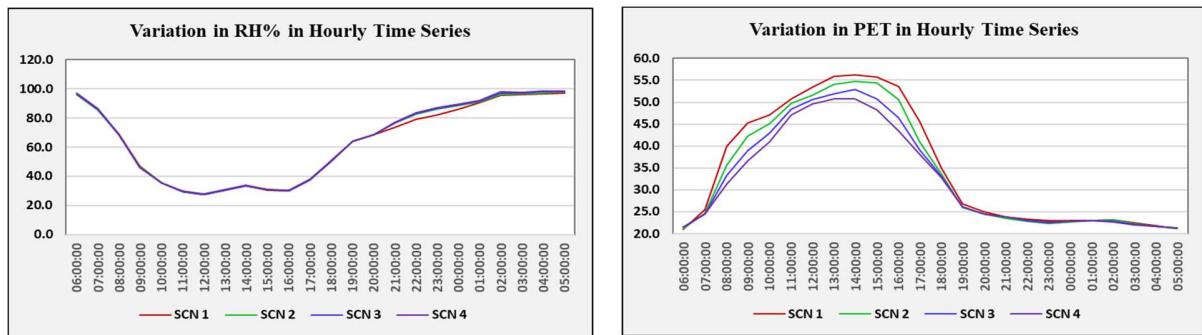


Figure 10: (Left) Scenario-wise comparative RH% variation in hourly time series and Figure 11: (Right) Scenario-wise comparative PET variation in hourly time series

Transposition of trend (Figure 12): Taking a closer look at the trend of change in PET across the scenarios it is found that in a selected time slot from 19:00 hrs. to 01:00 hrs. there is a transposition of trend in the scenario curves. The thermal comfort conditions in terms of mean PET values in SCN3 and SCN4 become worse in this time slot. In other words, when the building typology changes from mid-rise to high-rise, a dip in thermal comfort is observed which worsens as the typology further changes from high-rise to big high-rise (Figure 14).Further to understand the impact of UHI on the thermal comfort in OE, a scatter plot (Figure 13) of inflow boundary conditions of T_{air} with the ΔPET among scenarios was worked out. From the scatter plots it was concluded that the correlation of the two variables was stronger in the higher FSI scenario which implies that the impact of increased T_{air} due to the UHI effect will be intensified and the thermal conditions in the OE will worsen as the height of the built structures increases. Therefore,

the study supports the previous research that the aspect ratio has a strong effect on PET values; an increase in aspect ratio leads to lower daytime PET values though this reverses at night (Chatzidimitriou & Yannas, 2016).Temporal heat stress: Considering 35⁰C PET as the threshold value(Matzarakis&Amelung, n.d.), the duration of heat stress was analysed to understand the performance of various scenarios. In the SCN1 and SCN2 with low-rise and mid-rise built structures, the heat stress starts at 8:00 hrs. and continues till 17:00 hrs. It was further observed that there was a relief in the form of reduced duration of heat stress and a reduction in the highest recorded PET. In SCN3 and SCN4 the heat stress starts at 9:00 hrs and continues till 17:00 hrs. There is an average decrease of -4.99⁰C in the PET recorded between SCN1 to SCN4. The results of the present research are also in agreement with previous research which concluded that the increase in FSI and building heights reduces the duration of heat stress and

improves comfort conditions (Salal Rajan & Amirtham, 2021).

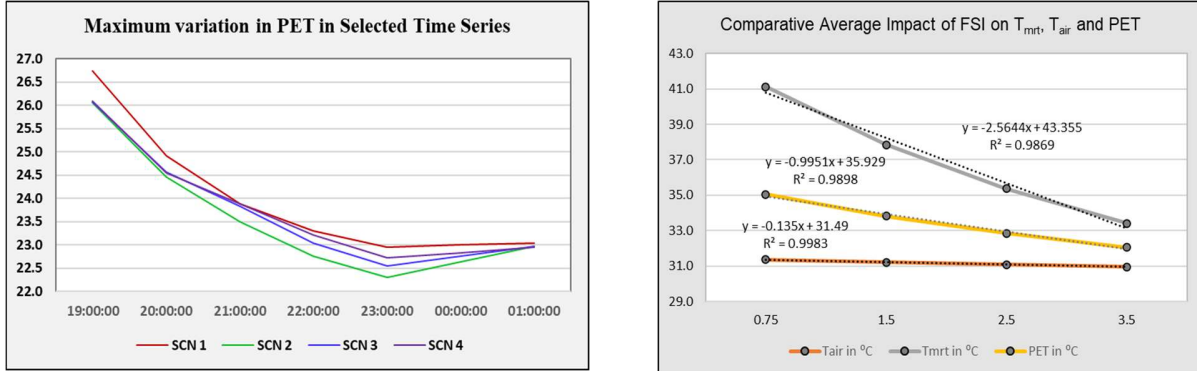


Figure 12: Chart showing the transposition of trend in the selected time slot and Figure 14: Comparative analysis of the regression of FSI on the average values of T_{air}, T_{mrt} and PET, on the simulation day

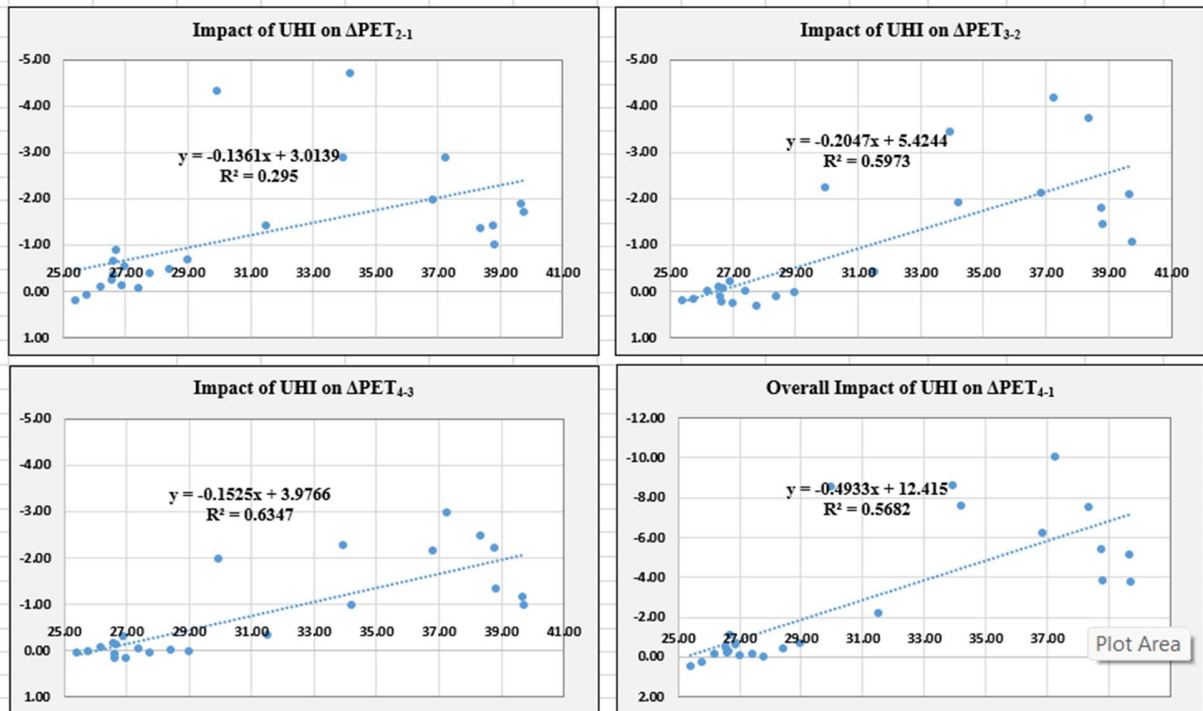


Figure 13: Scatter plots showing the impact of UHI on PET. (clockwise from the top left) change of SCN 1 to SCN 2, SCN 2 to SCN 3, SCN 1 to SCN 4 and SCN 3 to SCN 4

Further, the study of per-floor change in microclimate variables (Figure15) reveals that in the daytime the maximum impact is seen in T_{mrt} when the type of development changes from low rise to mid-rise, which gradually decreases as the building category changes to small and big high-rise. Since the observations are made at 1.5 m above ground level for all the categories, which corresponds to the height at which the microclimate

is experienced, the impact of change in building height beyond SCN3 gradually decreases. Change in T_{air} is not significant as compared to T_{mrt}. Change in PET is significant in the category shift of low rise to mid-rise, which becomes minor in the next category and slightly picks up in the big high-rise category. This change in the trend of PET is ascribed to the increased WS and RH%. In Figure15 it is seen that in the third category the

trend of change in WS and RH is positive which means that these two parameters are increasing with the additional floor heights in the higher FSI category. This helps to maintain the comfort conditions similar to the previous category in terms of similar PET levels, despite the increase in T_{air} and T_{mrt} . In the nighttime, the maximum impact is seen in T_{mrt} in the category change of low to mid-rise which slows down in the next category shift

and again becomes steeper in the big high-rise category. The trend of thermal comfort conditions in terms of PET reverses after midrise, which is more prominent at nighttime and becomes worse in the high-rise. The overall magnitude of change in T_{mrt} ($r=0.98, p=0.015$) was more as compared to the T_{air} ($r=0.99, p=0.005$). In high FSI, the duration of heat stress was reduced in the daytime. The high FSI shows better thermal comfort as measured in

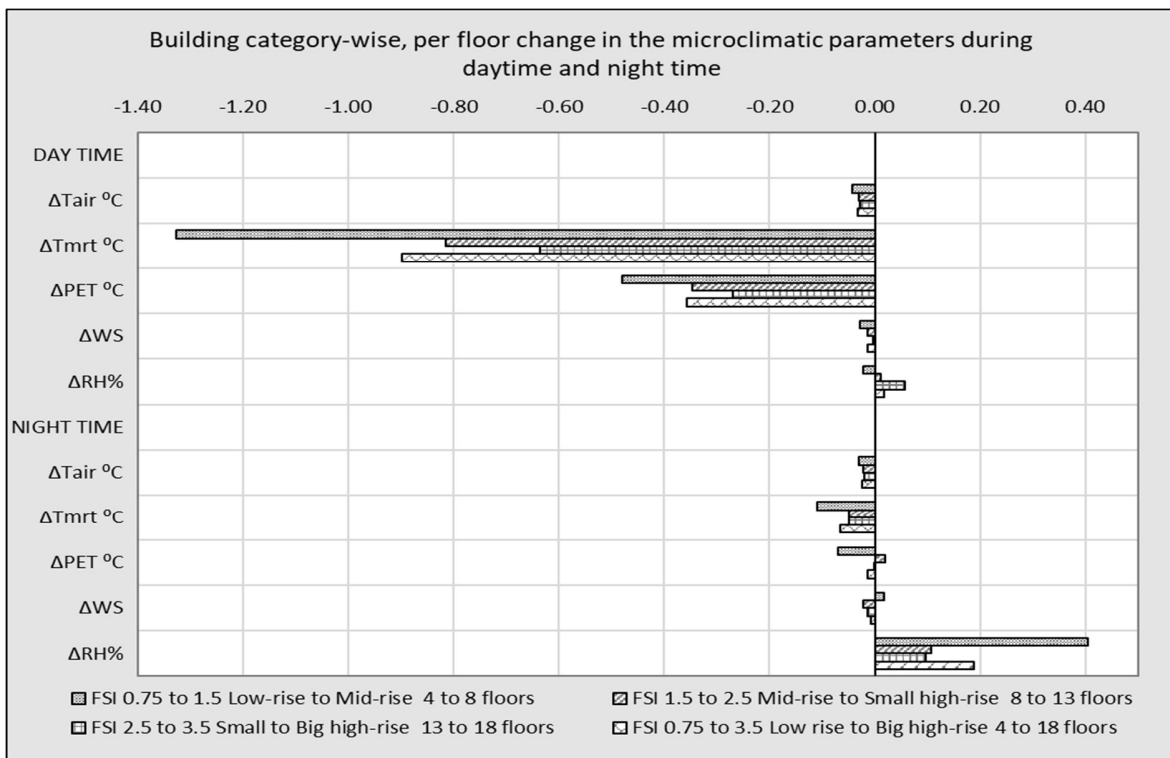


Figure 15: Building category-wise, per floor change in the microclimatic parameters

terms of PET, in the daytime but the trend was reversed in the late evening hours ie. from 20:00 to midnight. In this time slot, the PET was higher with the increase of FSI. There is a statistically significant relationship ($r= 0.98, p= 0.013$) between FSI and PET in °C. The analysis of WS and RH shows that a high FSI beyond 2.5, is more desirable due to the increased wind speed and relative humidity.

Conclusion

It is concluded that the scenarios with higher FSI reported low air temperature and mean radiant

temperature throughout the day. Also, in the high FSI scenario, it is found that the comfort conditions in the open space improved with the increase in WS and RH which can be attributed to the better shading and stack effect. Therefore, the present study concludes that higher FSI construction in the cities is more desirable as compared to low-density low FSI construction. Open spaces which are surrounded by buildings must be planned carefully to allow comfortable wind movements and maximize the shading effect. The regression equations (Figure 15) of each variable were derived considering the average values for the entire day. It will help planners to predict the impact of the

proposed FSI on the thermal comfort conditions of the open spaces enclosed by the built structures and achieve the desired values. The study concludes that the low FSI (up to 1.0) performs worst on account of thermal comfort, mid-FSI development (ranging from 1.0-2.5) is less desirable and high FSI development is found to be the best form of urban development. Since the boundary conditions and the morphological details of every research study done previously are different, therefore the results could not be compared directly. This study is specific to a particular type of layout in which the central open space is surrounded by the buildings at the periphery forming an open enclosure. It is applicable for the tropical monsoon type of climate

and specific range of FSI. Therefore, the impact of changing FSI may not be similar in other parts of the world with other types of climates. Further, there is a need to conduct similar studies with a greater number of FSI scenarios in different layouts to generalize the findings.

Acknowledgement

The corresponding author is thankful to Ar. Heena Patel for her constant technical support and valuable assistance in simulation, proofreading and other works related to the research.

Conflict of interest

The authors declare that they have no conflict of interest.

References

- Albdour, M. S., & Baranyai, B. (2019). An overview of microclimate tools for predicting the thermal comfort, meteorological parameters and design strategies in outdoor spaces. *Pollack Periodica*, 14(2), 109–118. <https://doi.org/10.1556/606.2019.14.2.10>
- Chatzidimitriou, A., & Yannas, S. (2004). Microclimatic Studies of Urban Open Spaces in Northern Greece. *The 21st Conference on Passive and Low Energy Architecture*. <https://www.researchgate.net/publication/254340558>
- Chatzidimitriou, A., & Yannas, S. (2016). Microclimate design for open spaces: Ranking urban design effects on pedestrian thermal comfort in summer. *Sustainable Cities and Society*, 26, 27–47. <https://doi.org/10.1016/j.scs.2016.05.004>
- Chatzinikolaou, E., Chalkias, C., & Dimopoulou, E. (2018). Urban microclimate improvement using ENVI-MET climate model. *International Archives of the Photogrammetry, Remote Sensing and Spatial Information Sciences - ISPRS Archives*, 42(4), 69–76. <https://doi.org/10.5194/isprs-archives-XLII-4-69-2018>
- Donny Koerniawan, M. (2015). *The Simulation Study of Thermal Comfort in Urban Open Spaces of Commercial Area Using EnviMet Software*. <https://www.researchgate.net/publication/281631147>
- Du, Y., Mak, C. M., & Tang, B. (2018). Effects of building height and porosity on pedestrian level wind comfort in a high-density urban built environment. *Building Simulation*, 11(6), 1215–1228. <https://doi.org/10.1007/s12273-018-0451-y>
- Emmanuel, R., Rosenlund, H., & Johansson, E. (2007). Urban shading - A design option for the tropics? A study in Colombo, Sri Lanka. *International Journal of Climatology*, 27(14), 1995–2004. <https://doi.org/10.1002/joc.1609>
- Erell, E., Pearlmutter, D., & Williamson, T. (2011). Urban Microclimate-Designing the Spaces between Buildings. *CITY WEATHERS: METEOROLOGY AND URBAN DESIGN 1950-2010*, 127–132.
- Fong, C. S., Aghamohammadi, N., Ramakreshnan, L., Sulaiman, N. M., & Mohammadi, P. (2019). Holistic recommendations for future outdoor thermal comfort assessment in tropical Southeast Asia: A critical appraisal. In *Sustainable Cities and Society* (Vol. 46). Elsevier Ltd. <https://doi.org/10.1016/j.scs.2019.101428>
- Jamei, E., Ossen, D. R., & Rajagopalan, P. (2017). Investigating the effect of urban configurations on the variation of air temperature. *International Journal of Sustainable Built Environment*, 6(2), 389–399. <https://doi.org/10.1016/j.ijsbe.2017.07.001>
- Jin, H., Liu, Z., Jin, Y., Kang, J., & Liu, J. (2017). The effects of residential area building layout on outdoor wind environment at the pedestrian level in severe cold regions of China. *Sustainability (Switzerland)*, 9(12). <https://doi.org/10.3390/su9122310>
- Kakon, A. N., Mishima, N., & Kojima, S. (2009). Simulation of the urban thermal comfort in a high-density tropical city: Analysis of the proposed urban construction rules for Dhaka, Bangladesh. *Building Simulation*, 2(4), 291–305. <https://doi.org/10.1007/s12273-009-9321-y>
- Kakoniti, A., Georgiou, G., Marakkos, K., Kumar, P., & Neophytou, M. K. A. (2016). The role of materials selection in the urban heat island effect in dry mid-latitude climates. *Environmental Fluid Mechanics*, 16(2), 347–371. <https://doi.org/10.1007/s10652-015-9426-z>
- Ketterer, C., & Matzarakis, A. (2015). Comparison of different methods for the assessment of the urban heat island in Stuttgart, Germany. *International Journal of*

- Biometeorology*, 59(9), 1299–1309. <https://doi.org/10.1007/s00484-014-0940-3>
- Koerniawan, M. D. (2017). The climate sensitive design in hot-humid urban design. *Dimensi (Journal of Architecture and Built Environment)*, 44(2). <https://doi.org/10.9744/dimensi.44.2.137-142>
- Lin, P., Lau, S. S. Y., Qin, H., & Gou, Z. (2017). Effects of urban planning indicators on urban heat island: a case study of pocket parks in high-rise high-density environment. *Landscape and Urban Planning*, 168, 48–60. <https://doi.org/10.1016/j.landurbplan.2017.09.024>
- Ma, T., & Chen, T. (2020). Classification and pedestrian-level wind environment assessment among Tianjin's residential area based on numerical simulation. *Urban Climate*, 34, 100702. <https://doi.org/10.1016/J.UCLIM.2020.100702>
- Matzarakis, A., & Amelung, B. (n.d.). *Physiological Equivalent Temperature as Indicator for Impacts of Climate Change on Thermal Comfort of Humans*. Springer Science + Business Media B.V. 2008.
- Mehrotra, S., Subramanian, D., Bardhan, R., & Jana, A. (2021). Effect of surface treatment and built form on thermal profile of open spaces: A case of Mumbai, India. *Urban Climate*, 35, 100736. <https://doi.org/10.1016/j.uclim.2020.100736>
- Nasir, R. A., Ahmad, S. S., Zain-Ahmed, A., & Ibrahim, N. (2015). Adapting Human Comfort in an Urban Area: The Role of Tree Shades Towards Urban Regeneration. *Social and Behavioral Sciences*, 170, 369–380. <https://doi.org/10.1016/j.sbspro.2015.01.047>
- Othman, H. A. S., & Alshboul, A. A. (2020). The role of urban morphology on outdoor thermal comfort: The case of Al-Sharq City – Az Zarqa. *Urban Climate*, 34, 100706. <https://doi.org/10.1016/J.UCLIM.2020.100706>
- Salal Rajan, E. H., & Amirtham, L. R. (2021). Impact of building regulations on the perceived outdoor thermal comfort in the mixed-use neighbourhood of Chennai. *Frontiers of Architectural Research*, 10(1), 148–163. <https://doi.org/10.1016/j.foar.2020.09.002>
- Salata, F., Golasi, I., Vollaro, A. D. L., & Vollaro, R. D. L. (2015). How high albedo and traditional buildings' materials and vegetation affect the quality of urban microclimate. A case study. *Energy and Buildings*, 99, 32–49. <https://doi.org/10.1016/j.enbuild.2015.04.010>
- Santamouris, M., Gaitani, N., Spanou, A., Saliari, M., Giannopoulou, K., Vasilakopoulou, K., & Kardomateas, T. (2012). Using cool paving materials to improve microclimate of urban areas - Design realization and results of the flisvos project. *Building and Environment*, 53, 128–136. <https://doi.org/10.1016/j.buildenv.2012.01.022>
- Shareef, S., & Abu-Hijleh, B. (2020). The effect of building height diversity on outdoor microclimate conditions in hot climate. A case study of Dubai-UAE. *Urban Climate*, 32, 100611. <https://doi.org/10.1016/J.UCLIM.2020.100611>
- Smith, C., & Levermore, G. (2008). Designing urban spaces and buildings to improve sustainability and quality of life in a warmer world. *Energy Policy*, 36(12), 4558–4562. <https://doi.org/10.1016/j.enpol.2008.09.011>
- Stocco, S., Cantón, M. A., & Correa, E. (2021). Evaluation of design schemes for urban squares in arid climate cities, Mendoza, Argentina. *Building Simulation*, 14(3), 763–777. <https://doi.org/10.1007/s12273-020-0691-5>
- Thakur, K. A., & Sanyal, A. J. (2016). Impact of Building by-laws on microclimatic elements of residential building layouts. Case Nagpur. *IOSR Journal of Environmental Science*, 10(11), 26–31. <https://doi.org/10.9790/2402-1011042631>
- Tumini, I., & Rubio-Bellido, C. (2016). Measuring Climate Change Impact on Urban Microclimate: A Case Study of Concepción. *Procedia Engineering*, 161, 2290–2296. <https://doi.org/10.1016/j.proeng.2016.08.830>
- Xue, F., Gou, Z., & Lau, S. S. Y. (2017). Green open space in high-dense Asian cities: Site configurations, microclimates and users' perceptions. *Sustainable Cities and Society*, 34, 114–125. <https://doi.org/10.1016/j.scs.2017.06.014>
- Yahia, M. W., & Johansson, E. (2013). Influence of urban planning regulations on the microclimate in a hot dry climate: The example of Damascus, Syria. *Journal of Housing and the Built Environment*, 28(1). <https://doi.org/10.1007/s10901-012-9280-y>
- Yang, J., Wang, Z. H., & Kaloush, K. E. (2015). Environmental impacts of reflective materials: Is high albedo a 'silver bullet' for mitigating urban heat island? In *Renewable and Sustainable Energy Reviews* (Vol. 47, pp. 830–843). Elsevier Ltd. <https://doi.org/10.1016/j.rser.2015.03.092>
- Yang, X., Zhao, L., Bruse, M., & Meng, Q. (2013). Evaluation of a microclimate model for predicting the thermal behavior of different ground surfaces. *Building and Environment*, 60, 93–104. <https://doi.org/10.1016/J.BUILDENV.2012.11.008>

Publisher's Note: ASEA remains neutral with regard to jurisdictional claims in published maps and figures.